# ■ Scientific Justification

We propose here an optimized snapshot program to find the first ever multiply-imaged supernova (SN). This program is now feasible on HST thanks to the dozens of galaxy clusters that now deep WFC3-IR imaging on well-modeled lens models. Along with the accompanying small GO follow-up program (PI:Strolger), we will use this unprecedented discovery to set the stage for the first ever use of a SN for time delay cosmography – a prospect initially conceived exactly fifty years ago (Refsdal, 1964). Even with just a single SN time delay, we will be able to measure H_0 to about 10% precision *without any reference to the local distance ladder.* This first SN time delay will therefore deliver a valuable test of systematic biases in other cosmological probes, and will serve as a pathfinder for future large samples of lensed SN (e.g. from LSST).

Motivation   As light from a distant source passes through a galaxy cluster, strong gravitational lensing causes multiple images to appear to the observer. The massive clusters in our target list all have dozens of multiple images known, and it is from these multiply imaged galaxies that we derive our primary constraints for cluster mass models (REFERENCE??). When a SN inevitably appears within one of these multiply-imaged galaxies, it will of course be multiply-imaged itself. Unlike the effectively static backgrond galaxies, a lensed SN is a transient source, so we will observe the multiple images appear to us separated by a time delay

$$\Delta t = \frac{(1 + z_L)}{c} \frac{D_L D_S}{D_{LS}} \phi, \quad (1)$$

$$\text{where } \phi = \frac{1}{2}(\theta - \beta)^2 - \psi(\theta), \quad (2)$$
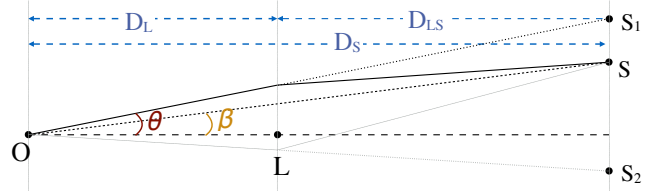
and z_L is the redshift of the lens, while D_L, D_S, and D_{LS} are angular diamater distances from the observer to the lens, observer to source, and lens to source, respectively. In Eq. 2 for the time delay potential (ϕ), the first term gives the geometric delay due to light rays following different path lengths to the observer, and the second term, ψ, is the relativistic component due to differing values of the gravitational potential along each path. The distance ratio $D_L D_S/D_{LS}$ in Eq. 1 carries a factor H_0^{-1}, so if the lensing potential ϕ is well known, this ***time delay cosmography provides a direct measurement of the Hubble constant – completely independent of the local distance ladder.***

After several decades of dedicated effort and slow progress, this field is now rapidly maturing (see Jackson, 2007; Treu, 2010, for recent reviews). The complete sample comprises $\sim$20 time delay measurements, exclusively from *quasars.* These are typically lensed by a single foreground galaxy, with only a few magnified by galaxy clusters (Inada et al., 2003, 2006; Oguri et al., 2008; Dahle et al., 2013). As techniques for measuring the time delay Δt and modeling the lensing potential ψ have improved, there are now a few of these lensed quasars that can jointly deliver an H_0 constraint with $\sim$6% precision (e.g. Suyu et al., 2010, 2013). The distances derived from these time delay measurements are particularly complementary

to high-z cosmological probes like the Cosmic Microwave Background (CMB; Linder, 2011). Time delay distances provide an especially powerful check for unknown systematics, because – unlike SN Ia– each separate time delay measurement can be individually quite precise and largely independent of the rest of the sample (Suyu et al., 2013; Treu et al., 2013). *A measured time delay from even a single multiply-imaged SN would be a valuable addition, and would provide a critical first step towards future samples with over 100 SN time delays in the LSST era.*

A cluster-lensed SN would provide several distinct advantages that make such an object particularly attractive for time delay cosmography. First, the age of a SN relative to explosion can be measured to within ± 3 days from light curve shape and color, or from spectroscopic cross-correlation (Filippenko, 1997; Blondin & Tonry, 2007). Thus the time delay measurement does not require continuous long-term monitoring, as is needed for precise quasar time delay measurements (e.g. Fohlmeister et al., 2013; Tewes et al., 2013b). Furthermore, with a cluster as the lensing object instead of a single galaxy, there is a much lower likelihood of microlensing from intervening compact objects (stars), and the microlensing effect can be more easily disentangled from a SN light curve than from a quasar (Kolatt & Bartelmann, 1998; Tewes et al., 2013a). Finally, if the lensed object is a Type Ia SN (SN Ia), then the luminosity distance can be independently constrained using light curve fitting (Phillips, 1993). Some very recent work has even suggested that it might also be possible to measure luminosity distances from Type II-P SN light curves, though with lower precision (Anderson et al., 2014; Sanders et al., 2014). With a known luminosity distance, the source magnification can be directly measured, providing powerful additional leverage for breaking degeneracies in the lens model (Kolatt & Bartelmann, 1998; Oguri & Kawano, 2003).

Predicted Yield   To estimate the number of snapshots we need, we start with a tabulation of the number of known multiply-imaged galaxies in the fields of our target clusters (Table 1 ** we need to list the number of images, maybe not only the useful fraction?). This is a conservative approach, as it is quite possible to detect a multiply-imaged SN even if the host galaxy is well below the current detection thresholds for these cluster fields. The total yield of strongly-lensed SN per snapshot is $N_{SN} = SNR_M \times M_{gal} \times N_{gal} \times t_{vis}$. Here SNR_M is the SN rate per unit mass, M_{gal} is the average mass of a multiply-imaged galaxy, N_{gal} is the number of multiply imaged galaxies in the field, and t_{vis} is the length of time that any given SN is visible to our snapshot survey.

Most of the lensed systems in our target list are at $z \sim 2$, in an era near the peak of the cosmic star formation history, so we assume that our average lensed galaxy is generating SN at a rate similar to an Sc galaxy in our local universe: $SNR_M \sim 0.2(100\mathrm{yr})^{-1}(10^{10}\mathrm{M_\odot})^{-1}$ for SN Ia and $0.7(100\mathrm{yr})^{-1}(10^{10}\mathrm{M_\odot})^{-1}$ for Type II (Mannucci et al., 2005). We adopt an average stellar mass of $M_{gal} = 10^{10.7}\mathrm{M_\odot}$ (Tomczak et al., 2014), and use the census of multiply-imaged systems in Table 1 to predict an average of $N_{gal} \sim 35$ lensed galaxy images per cluster[2]. Using simulated SN light curves in 240 multiply-imaged galaxies (Figure 1), we

[2]Note that we count each separate image of a multiple-image set except the last one (one

find an average $t_{vis} \sim 30$ days for SN Ia and ~ 20 days for SN II.

With these relatively conservative estimates, we get $N_{SN} \sim 0.1$ SN per snapshot, including both Type Ia and II. To give this program a good chance at discovering a strongly lensed SN in Cycle 22, we request 200 snapshots. Assuming a realistic snapshot execution rate of $\sim 30\%$, this program should yield a sample of $\sim 6 \pm 4$ SN in one year. Even if our yield prediction is biased high by a factor of ~ 2, we still have a better than 68% chance to catch at least one. Given the intrinsic value of each lensed SN, even just a single detection will nevertheless be an extraordinary step forward for time delay cosmography.

Finally, we note that this snapshot program is designed mainly for discovery. Follow-up observations will come from accompanying GO program (PI: Strolger), using 12 orbits with ToO observations for immediate confirmation of a SN candidate and measurement of the light curve. Sometime in the future, a return campaign to catch the next image would be needed to complete the time delay measurement, using HST, ground-based AO systems, or possibly JWST, depending on the length of the delay.

▉ Description of the Observations

In Cycle 22, HST has just achieved a new capability for the discovery of a multiply-imaged SN. Three key ingredients will make this program feasible for the first time in this cycle: (1) the use of WFC3-IR, (2) a SNAP survey strategy with repeated shallow visits over many clusters, and (3) a carefully optimized target list of clusters with both IR template imaging and excellent mass models.

1. WFC3-IR: Ground-based surveys and even HST/ACS programs have looked for lensed SN (e.g. Sharon et al., 2007; Dawson et al., 2009; Sharon et al., 2010; Sand et al., 2011), but none of these have had the capability to detect SN at $z \sim 2$, even with substantial magnification, so many multiply-imaged galaxies were effectively unreachable to them. Amanullah et al. (2011) demonstrated the value of searching for high-z SN at IR wavelengths, where you sample rest-frame optical bands at the peak of the SN SED. Using a K-band survey from the VLT with HAWK-

Table 2: Detection Limits

WFC3/IR Filter	Exp. Time [min]	m_{lim} [*] [AB mag]
F110W	12	26.3
F110W	20	26.6
F110W	30	26.9
F140W	12	25.9
F140W	20	26.2
F140W	30	26.5

[*] Apparent magnitude that yields S/N of 5 (optimum S/N$\sim$10) in the given exposure time.

I[1] they discovered of a lens-magnified SN at $z \sim 1.7$ behind the galaxy cluster Abell 1689. With the CANDELS and CLASH programs, we have taken this IR search strategy above the atmosphere, showing that WFC3-IR is capable of discovering even un-lensed SNe at $z > 1.5$ (Rodney et al., 2012; Jones et al., 2013), and finding three more lens-magnified

cannot measure a time delay from the last appearance). The time delay between each image is of order months or years, so each snapshot is essentially observing the same galaxy at several widely-spaced epochs that can be treated as independent.

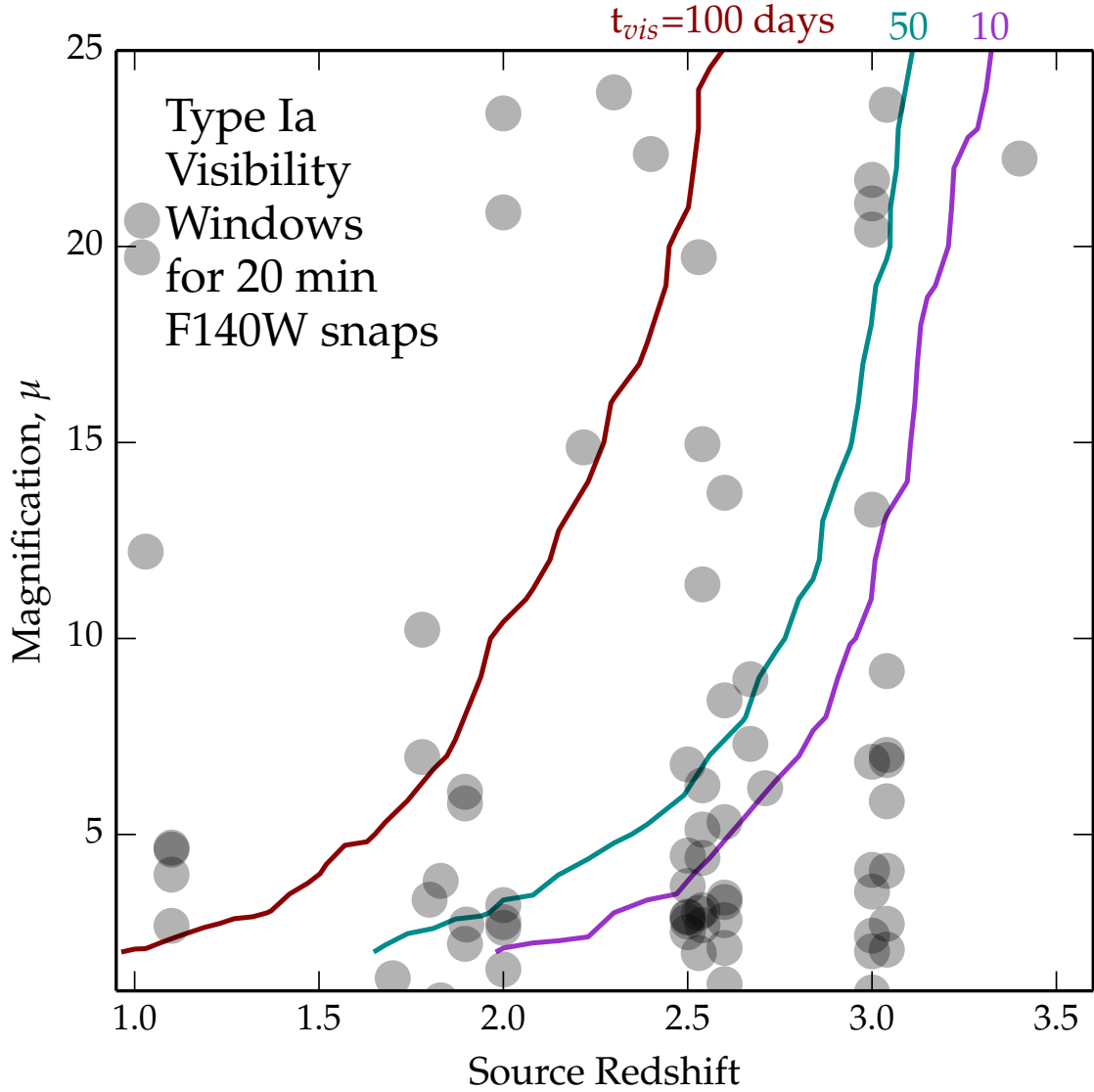[1]VLT: Very Large Telescope; HAWK-I: High Acuity Wide-field K-band Imager

Figure 1: Visibility time contours in the redshift-magnification plane. Using simulated light curves of an average lensed Type Ia SN, we have measured the expected visibility window (a.k.a the control time): the number of days that the SN is above our detection threshold for a 20-minute snapshot. Solid lines plot contours of constant visibility time in the $z - \mu$ plane at $t_{vis} =$100, 50, and 10 days. Grey points mark the measured magnifications and redshifts for 50 strongly-lensed galaxy images from three of our primary cluster targets.

Table 1: Cluster Target List

Cluster	R.A.	Decl.	z	N_{im} *	References
Abell 2744[†]	00:14:23.4	-30:23:26	0.31	43	Merten et al. 2011
CL0024	00:26:35.0	+17:09:43	0.39	20	Zitrin et al. 2009a
El Gordo	01:02:52.5	-49:14:58	0.87	11	Zitrin et al. 2013b
Abell 370[†]	02:39:52.8	-01:34:36	0.37	36	Richard et al. 2009, ZFF
Abell 383	02:48:03.4	-03:31:44	0.19	18	Zitrin et al. 2011b
MACS0416[†]	04:16:08.4	-24:04:21	0.40	36	Zitrin et al. 2013
MACS0647	06:47:50.3	+70:14:55	0.58	20	Zitrin et al. 2011, Coe et al. 2013
Bullet-a	06:58:37.9	-55:57:00	0.3	10	Bradac et al. **
Bullet-b	06:58:37.9	-55:57:00	0.3	11	Bradac et al. **
MACS0717-a	07:17:35.6	+37:44:44	0.55	18	Zitrin et al. 2009b, Limousin et al. 2012, Z14
MACS0717-b	07:17:35.6	+37:44:44	0.55	18	Zitrin et al. 2009b, Limousin et al. 2012, Z14
MACS0744	07:44:52.8	+39:27:24	0.70	14	Zitrin et al. 2011; 2014 in prep
Abell 611	08:00:56.8	+36:03:23	0.21	12	Newman et al. 2013, Z14
MACS1149[†]	11:49:35.7	+22:23:55	0.54	29	Zitrin & Broadhurst 2009, Zheng et al. 2012
MACS1206[†]	12:06:12.1	-08:48:04	0.44	33	Ebeling et al. 2009, Zitrin et al. 2012
Abell 1689[†]	13:11:34.2	-01:21:56	0.19	117	Broadhurst et al. 2005, Coe et al. 2010, Diego et al.
Abell 1703[†]	13:15:03.7	+51:49:27	0.28	36	Limousin et al. 200*, Zitrin et al. 2010
RXJ1347	13:47:31.1	-11:45:12	0.45	14	Köhlinger & Schmidt 2014
MS1358	13:59:48.7	+62:30:48	0.33	13	Zitrin et al. 2011c
Abell 1835	14:01:02.0	+02:52:45	0.25	17	Richard et al. 2010, Morandi et al. 2012
Abell 2218	16:35:54.0	+66:13:00	0.18	18	Kneib et al. 2004
Abell 2261	17:22:27.2	+32:07:57	0.22	18	Coe et al. 2012
MACS1931	19:31:49.6	-26:34:32	0.35	10	Z14
MACS2129	21:29:26.1	-07:41:28	0.57	14	Zitrin et al. 2011; Z14
RXJ2248[†]	22:48:44.0	-44:31:51	0.35	28	Monna et al. 2013

* Approximate number of known strongly-lensed galaxy images within the WFC3-IR FOV, counting all instances of each lensed galaxy except the last (i.e. all independent lensed galaxy images that could deliver a SN time delay measurement).
† Primary targets. We will allocate more snapshots to these clusters that have especially strong lenses with many multiply-imaged galaxies and particularly good lens models. The unweighted average N_{im} is ~25, but we expect this weighted snapshot allocation to result in an actual mean of $N_{im} \sim 35$.

SNe (Patel et al., 2013; **?**). The ongoing Hubble Frontier Fields (HFF) program (PI:Lotz) is gathering deep WFC3-IR imaging of 6 galaxy clusters, and with our multi-cycle GO program (PI:Rodney) we have already found 8 SN in the HFF data, including 2 with significant magnification. However, all of these magnified SN are too far away from the cluster center to be multiply-imaged.

2. Snapshots: A primary reason that recent WFC3-IR surveys have not found any multiply-imaged SN is because they are optimized for depth and wavelength coverage instead of cadence. CLASH, for example, collected WFC3-IR imaging of 25 clusters over 3 years, but many orbits were allocated to ACS and WFC3-UVIS, and the time separation between the first and last IR image on any single cluster was typically only ∼40 days. Thus, in practice each cluster only had one epoch suitable for a lensed SN search, making any detection extremely unlikely. The HFF program only exacerbates this problem, by drilling even deeper on a much smaller number of clusters. However, CLASH, HFF and other programs have now provided deep IR template imaging of many massive clusters from which to construct difference images for SN discovery. Our snapshot program will capitalize on this rich archival treasury by delivering hundreds of shallow visits across ∼25 clusters, covering a long time baseline to maximize our chance of catching a multiply-imaged SN in action.

3. Cluster Target Selection: The HST archive now holds a deep trove of ACS and (most notably) WFC3-IR imaging on strong-lensing galaxy clusters at redshifts $z \sim 0.2 - 0.7$. This valuable data set has led to an explosion of high quality cluster lens models, thanks to much effort in supplemental observations and modeling (e.g. Kneib et al., 2004; Smith et al., 2005; Limousin et al., 2008; Bradač et al., 2008; Richard et al., 2009). Co-PI Zitrin has had a leading role in this recent burst, principally through the light-traces-mass (LTM) lens modeling technique, which particularly excels with its predictive power for the discovery of multiply-imaged galaxies (Broadhurst et al., 2005; Zitrin et al., 2009b). Through the CLASH program, this approach is being used to generate precise mass models for 25 clusters, dramatically expanding the number of well-studied strong-lensing clusters with many multiple-image systems (e.g. Zitrin et al., 2009b,a, 2011a,b,c; Merten et al., 2011; Zitrin et al., 2012a,b, 2013b,a; Coe et al., 2012, 2013). The quality of our lens models will translate directly into the uncertainty in our determination of H_0. We find that reaching ∼10% precision on H_0 is a very plausible benchmark, consistent with past estimates (?Oguri & Kawano, 2003; Riehm et al., 2011).

To build our target list, we have taken into account the trade-off between the number of lensed galaxies and the length of their time delays. Very massive clusters will generally provide more multiply-imaged background galaxies that could host a SN during our survey. However, very massive clusters will also on avarage yield time delays which are too long to be of practical use hard to measure on a reasonable time scale (Δt can be $\sim 10^3$ years). In some cases as few as $\sim 10 - 20\%$ of the multiple-image pairs behind these monster lenses would yield desirable time delays on the scale of months to years. Therefore, the optimal cluster lens targets are medium-to-large lenses with Einstein radii of roughly $\sim 10 - 30''$. There is also some dependence on the exact structure and redshift of the lens, but as a rule of thumb such lenses will each have about 5-20 multiple galaxy images with useful time delays.

Table 1 presents our list of 25 cluster targets, which are spread across the sky to optimize snapshot observability. The list is dominated by lenses of moderate strength, but supplemented with 2-3 more massive clusters that contain of order 100 multiple images each.

■ **Special Requirements**

■ **Justify Duplications**

References

Amanullah, R., et al. 2011, ApJ, 742, L7
Anderson, J. P., et al. 2014, ArXiv e-prints
Blondin, S., & Tonry, J. L. 2007, ApJ, 666, 1024
Bradač, M., et al. 2008, ApJ, 687, 959
Broadhurst, T., et al. 2005, ApJ, 621, 53
Coe, D., et al. 2012, arXiv eprint, 1201.1616
—. 2013, ApJ, 762, 32
Dahle, H., et al. 2013, ApJ, 773, 146
Dawson, K. S., et al. 2009, AJ, 138, 1271
Filippenko, A. V. 1997, ARA&A, 35, 309
Fohlmeister, J., et al. 2013, ApJ, 764, 186
Inada, N., et al. 2006, ApJ, 653, L97
—. 2003, Nature, 426, 810
Jackson, N. 2007, Living Reviews in Relativity, 10, 4
Jones, D. O., et al. 2013, ApJ, 768, 166
Kneib, J.-P., et al. 2004, ApJ, 607, 697
Kolatt, T. S., & Bartelmann, M. 1998, MNRAS, 296, 763
Limousin, M., et al. 2008, A&A, 489, 23
Linder, E. V. 2011, Phys. Rev. D, 84, 123529
Mannucci, F., et al. 2005, A&A, 433, 807
Merten, J., et al. 2011, MNRAS, 417, 333
Oguri, M., & Kawano, Y. 2003, MNRAS, 338, L25
Oguri, M., et al. 2008, ApJ, 676, L1
Patel, B., et al. 2013, ApJ, submitted (arXiv:1312.0943)
Phillips, M. M. 1993, ApJ, 413, L105
Refsdal, S. 1964, MNRAS, 128, 307
Richard, J., et al. 2009, A&A, 498, 37
Riehm, T., et al. 2011, A&A, 536, A94
Rodney, S. A., et al. 2012, ApJ, 746, 5
Sand, D. J., et al. 2011, ApJ, 729, 142
Sanders, N. E., et al. 2014, ArXiv e-prints
Sharon, K., et al. 2010, ApJ, 718, 876
Sharon, K., et al. 2007, ApJ, 660, 1165
Smith, G. P., et al. 2005, MNRAS, 359, 417
Suyu, S. H., et al. 2013, ApJ, 766, 70
—. 2010, ApJ, 711, 201
Tewes, M., Courbin, F., & Meylan, G. 2013a, A&A, 553, A120
Tewes, M., et al. 2013b, A&A, 556, A22
Tomczak, A. R., et al. 2014, ApJ, 783, 85
Treu, T. 2010, ARA&A, 48, 87
Treu, T., et al. 2013, ArXiv e-prints
Zitrin, A., et al. 2011a, MNRAS, 410, 1939
—. 2011b, MNRAS, 413, 1753
—. 2011c, ApJ, 742, 117
—. 2009a, ApJ, 707, L102
—. 2009b, MNRAS, 396, 1985
—. 2013a, ApJ, 770, L15
—. 2013b, ApJ, 762, L30
—. 2012a, ApJ, 747, L9
—. 2012b, ApJ, 749, 97

Table 3: Past HST Usage for co-PIs

PID	Title	PI
12060-64, 12440-45	CANDELS	Cycle 18-20 MCT
12065-69, 12100-04, 12451-60	CLASH	Cycle 18-20 MCT
12099, 12461, 13063	C+C SN Follow-up	Cycle 18-20 MCT
13046	RAISIN	Cycle 20 ToO; collecting data
13279	Characterizing the Young Galaxies at Cosmic Dawn	Zheng (JHU); archival
13317	Infrared Grism Confirmation of a Strongly Lensed z~11 Candidate: MACS0647-JD	Coe (STScI)
13386	Frontier Field Supernova Search	Rodney (JHU); archival
13236	Galaxy Evolution at the Frontier	Bradley (STScI); archival
$\cdots$	Frontier Fields Map Making	Zitrin & Merten (2013)

* Listed publications are those with direct input from PI's Rodney and Zitrin, and the CANDELS/CLA

Past HST Usage

Table 3 lists the HST programs from recent cycles that include one or both co-PIs Rodney and Zitrin.